

Contents lists available at ScienceDirect

Polymer

journal homepage: www.elsevier.com/locate/polymer



NMR spectroscopic characterization of polyhalodisulfides via sulfenyl chloride inverse vulcanization with sulfur monochloride

Chisom Olikagu ^a, Vlad K. Kumirov ^a, Jon T. Njardarson ^a, Megan J. Hahn ^a, Jeffrey Pyun ^{a,b,*}

ARTICLE INFO

Keywords: Sulfenyl chlorides Sulfur monochloride Step-growth polymerization NMR spectroscopy

ABSTRACT

The preparation of sulfur containing polymers from inexpensive, commodity sulfur base chemicals is an emerging field of polymer chemistry as a route to consume elemental sulfur generated from fossil fuel refining. Recently a new process, termed, sulfenyl chloride inverse vulcanization has been developed that exploits the high reactivity and miscibility of sulfur monochloride, (S₂Cl₂) with a broad range of allylic monomers to prepare soluble, high molar mass linear polymers, segmented block copolymers and crosslinked thermosets with greater synthetic precision than achieved using classical inverse vulcanization with elemental sulfur. However, the ringopening of episulfonium intermediates from this polymerization can proceed via Markovnikov, anti-Markovnikov, or alternative pathways resulting in complex regioisomeric microstructures, particularly when used with allylic ester monomers. Hence, to accelerate structural characterization of this new class of polyhalodisulfides prepared by the sulfenyl chloride inverse vulcanization process, we report on a detailed structural characterization to quantify the molar composition of regioisomeric units in these materials using NMR spectroscopy, focusing on sulfenyl chloride additions to allylic benzoate substrates. We report on a general methodology using one- and two-dimensional NMR spectroscopic techniques to enable direct integration of 2D NMR spectroscopic cross peaks to quantify the molar composition of regioisomeric units in 1,3-diallyl isophthalate (DAI) polymerized with S2Cl2, along with detailed studies on model compound reactions to detail the analytical methodology.

1. Introduction

The use of wholly inorganic sulfenyl chlorides, such as, sulfur monochloride (S_2Cl_2) as a feedstock for polymeric materials also has significant potential as a route to utilization of elemental sulfur stockpiles that are generated in enormous volume via petroleum refining [1]. Polymerization of elemental sulfur (S_8) has emerged in the past decade as an important new area of polymer chemistry and sustainable polymer science [2–6]. This new area has been driven by the discovery of the inverse vulcanization process by Pyun et al. [7] in 2013 using molten elemental sulfur for free radical polymerizations with unsaturated organic comonomers. While this new chemical polymerization has proven to be significant, the narrow scope of miscible organic monomers in liquid sulfur, along with the high temperatures required for this process, has limited the scope of new inverse vulcanized organopolysulfides that have been developed. This has prompted the use of inverse vulcanized polysulfide resins to be used for further

post-polymerization reactions via *Dynamic Covalent Polymerizations*, [8] along with the use of organic accelerators [9,10], or transition metal complex based catalysts [11,12] for inverse vulcanization. The use of other commodity chemicals derived from elemental sulfur (e.g., sulfur base chemicals) have also been explored as monomers for polymer synthesis as an alternative approach to sulfur utilization, which include sulfur commodity chemicals, such as, carbon disulfide (CS₂) and sulfenyl chlorides. The synthesis and polymerization of well-defined, soluble chalcogenide rich monomers has been demonstrated by Pople et al. on the synthesis and electrochemical polymerization of cyclic trisulfides derived from S_8 [13].

Wholly inorganic families of chalcogenide halides, which include sulfur dichloride (SCl_2) and sulfur monochloride (S_2Cl_2) have been widely used and readily add to unsaturated olefinic molecules [14,15]. S_2Cl_2 has numerous chemical advantages for synthetic chemistry vs S_8 , namely, the *excellent miscibility with conventional organic media and organic comonomers* in stark contrast to liquid elemental sulfur. S_2Cl_2 has

^a Department of Chemistry and Biochemistry, University of Arizona, Tucson, AZ, 85721, United States

^b James C. Wyant College of Optical Sciences, University of Arizona, Tucson, AZ, 85721, United States

^{*} Corresponding author. Department of Chemistry and Biochemistry, University of Arizona, Tucson, AZ, 85721, United States. *E-mail address*: jpyun@email.arizona.edu (J. Pyun).

a long history of use in crosslinking/vulcanization of natural rubber, styrene-butadiene rubber, and butyl rubber, where sulfenyl chlorides are significantly more reactive than elemental/insoluble sulfur and must be done at room temperature (RT) to form crosslinked rubber, which is referred to as "cold vulcanization." [16,17] There have been only a handful of scientific publications on the use of sulfur monochloride as a comonomer for making polymers, which include copolymerizations with olefinic compounds. However, these early reports from the 1960's by Schmid, Meyer and Lautenschlager, primarily afforded oligomers from cyclic olefinic compounds [18–23]. Copolymerization of S_2Cl_2 with diamine and bis-anilino compounds has recently been revised as a new step-growth polymerization process to prepare poly(amino sulfides). However, due to the reduced bond strength of S-N bonds, these polyaminosulfides have primarily been targeted for degradable scaffolds for drug delivery [24,25]. The propensity of these inorganic, or organosulfenyl chloride groups to undergo intramolecular cyclization reactions to electrophilic moieties (e.g., arenes) has been widely exploited for the synthesis of heterocyclic small molecules [14,15], but is problematic for linear, or network step-growth polymerization reactions, as cyclization side-reactions limit monomer conversion and lead to oligomeric

To exploit the high reactivity and commercial availability of S₂Cl₂ industrially, Pyun et al., developed a new process, termed, sulfenyl chloride inverse vulcanization (SC-IV) [1], which is an addition step-growth polymerization of S₂Cl₂ with allylic monomers which was successfully applied to prepare a new class of polymers (polyhalodisulfides), where a wide range of soluble, high molar mass linear polymers, segmented block copolymers, and glassy crosslinked thermosets were synthesized from this new polymerization. This methodology enabled the application of classical molecular monomer architectures from step-growth polymerization (e.g., terephthalates, isophthalates, bis-phenols and isocyanurates) to sulfenyl chloride inverse vulcanization processes, which was a major advance over classical inverse vulcanization with S₈. A key mechanistic feature of SC-IV is the formation of episulfonium intermediates formed after electrophilic addition of the R-S-Cl group to the olefinic monomer groups. The electrophilic addition can proceed with either Markovnikov, anti-Markovnikov, or other mechanistic pathways which affords a regioisomeric mixture of polymer microstructures in the final material. Structural analysis of these polymer microstructures was conducted by solution one-dimensional (1-D) and two-dimensional (2-D) NMR spectroscopy, in particular, quantitative 2-D Heteronuclear Single Quantum Coherence spectroscopy (HSOC) [1]. This analysis was particularly important for structure characterization of the polyhalodisulfides prepared by the SC-IV of S₂Cl₂ with 1,3-diallyl isophthalate (DAI), where the allyl benzoate fragments of DAI led to other regioisomeric microstructures via intramolecular ring-opening of episulfonium intermediates.

Herein, we report the solution NMR spectral assignments for polyhalodisulfides made from the sulfenyl chloride inverse vulcanization of S₂Cl₂ with 1,3-diallyl isophthalate (DAI) using both 1D and 2D NMR spectroscopic techniques, namely, heteronuclear single quantum coherence spectroscopy (HSQC). In particular, we report on the use of small molecule model compounds for both sulfenyl chlorides and DAI to enable detailed instruction on the NMR spectroscopic analytic methodology used to quantify the polymer microstructures observed in this polymerization. Due to the complexity of regioisomers formed in the SC-IV process with allylic monomers, this report is timely in offering guidance on the NMR spectroscopic characterization of soluble polyhalodisulfides made via SC-IV without the need for model compounds, or supporting NMR spectroscopic methods (e.g., solid state measurements). Although the application of 2D NMR HSQC spectroscopy data for quantitative analysis is not widely used, the relative integration of cross peaks for molar ratio quantitation is feasible as have been widely reported [26]. The primary objective of this report is to delineate accelerated methods for structural characterization

polyhalodisulfides prepared by SC-IV. A $(^{1}H^{-13}C)$ -HSQC spectrum shows ^{1}H signals separated by the chemical shift of their attached carbons which allows for more accurate integration of specific ^{1}H signals in an overlap region especially with mixtures, while the ^{13}C chemical shift is used to identify different carbon groups in the polymer. It is also important to note the benefits of rapid HSQC spectra acquisition time, as all the data presented herein require only 5 min to acquire.

2. Results & discussion

The addition of organosulfenyl chlorides (RS-Cl) to terminal olefins is characterized by the formation of an episulfonium ring, followed by Markovnikov or anti-Markovnikov addition of the chloride ion to either carbon of the episulfonium ring resulting in regio- and stereoisomeric mixtures (Scheme 1) [1,14,15]. Nevertheless, this facile electrophilic addition to terminal olefins is highly efficient and does not form small molecule byproducts, enabling both solution and bulk reaction conditions to be applied.

Poly(S2-DAI-Cl2) is a polyhalodisulfide synthesized by the sulfenyl chloride inverse vulcanization of DAI and S₂Cl₂ which proceeds through the episulfonium intermediates presented in Scheme 1. Hence the microstructure of this polymer affords regioisomers, which we previously characterized by quantitative 2D HSQC NMR spectroscopy. Since future design improvements of polymer properties requires more precise structure-property correlations, we delved deeper into structural characterization of these polymers where we conducted rigorous 1D and 2D NMR spectroscopic studies on small molecule model compounds towards characterization of poly(S₂-DAI-Cl₂) (Scheme 2a-c). In this study, we analyzed the product mixture obtained from the monofunctional analogue of DAI (allyl benzoate) and a monofunctional sulfenyl chloride (phenyl sulfenyl chloride, Ph-SCl), along with S2Cl2 as the difunctional sulfenyl chloride, to garner insight to the microstructure of poly(S2-DAI-Cl₂) (Scheme 2a, 2b). SC-IV of DAI and S₂Cl₂ was observed to form both Markovnikov, anti-Markovnikov, and a third regioisomeric microstructure (dihydrodioxolium), hence, the model reaction of allyl benzoate with S₂Cl₂ was significant to confirm if the dihydrodioxolium regioisomeric pathway was also observed and characteristic of R-S-Cl addition to allylic ester substrates.

The proposed mechanism leading to the formation of Markovnikov, anti-Markovnikov, and regioisomeric dihydrodioxolium products (Scheme 2b), or regioisomeric polymer microstructures (Scheme 2c) is shown in Fig. 1. The Markovnikov isomeric fragment (pathway I; Fig. 1) is formed by attack of the chloride anion to the hindered carbon of the episulfonium forming methine -CH-Cl and methylene -CH₂S- fragments, while the anti-Markovnikov addition (pathway II, Fig. 1) affords methylene -CH2Cl and methine -CH-S- fragments. Furthermore, addition of the neighboring carbonyl oxygen atom to the less hindered carbon of episulfonium intermediate afforded a six-membered dihydrodioxolium cyclic intermediate which after chloride anion attack affords a methylene -CH₂Cl and methine -CH-S- fragments (pathway III, Fig. 1) identical to the fragments formed from anti-Markovnikov pathway II, rendering these pathways II and III as indistinguishable from structural analysis only. Finally, addition of the neighboring carbonyl oxygen atom to the more hindered carbon of episulfonium intermediate afforded a five-membered dihydrodioxolium cyclic intermediate which after chloride anion attack (pathway IV, Fig. 1) affords a new regioisomer of both methylene -CH2Cl and methylene -CH2-Sfragments.

The structural analysis of these possible products was further complicated by the use of difunctional sulfenyl chlorides, such as S_2Cl_2 , affording multiple dimeric products yielding six distinct regioisomeric products from the Markovnikov, anti-Markovnikov, or dihydrodioxolium pathways (Fig. 2). Since each possible regioisomeric product consisted of two chiral centers along with diastereotopic protons, the 1D 1 H NMR spectrum of these product mixtures were complex and often overlapped, requiring the use of 2D HSQC NMR spectroscopy,

Scheme 1. General reaction scheme for addition reactions of monofunctional sulfenyl chlorides to alpha olefins.

Scheme 2. (a) synthetic scheme for electrophilic addition of phenyl sulfenyl chloride to allyl benzoate, (b) synthetic scheme for electrophilic addition of sulfur monochloride to allyl benzoate as a model reaction for SC-IV of DAI and S_2Cl_2 , (c) synthesis of poly (S_2 -DAI- Cl_2) from SC-IV of diallyl isophthalate and sulfur monochloride.

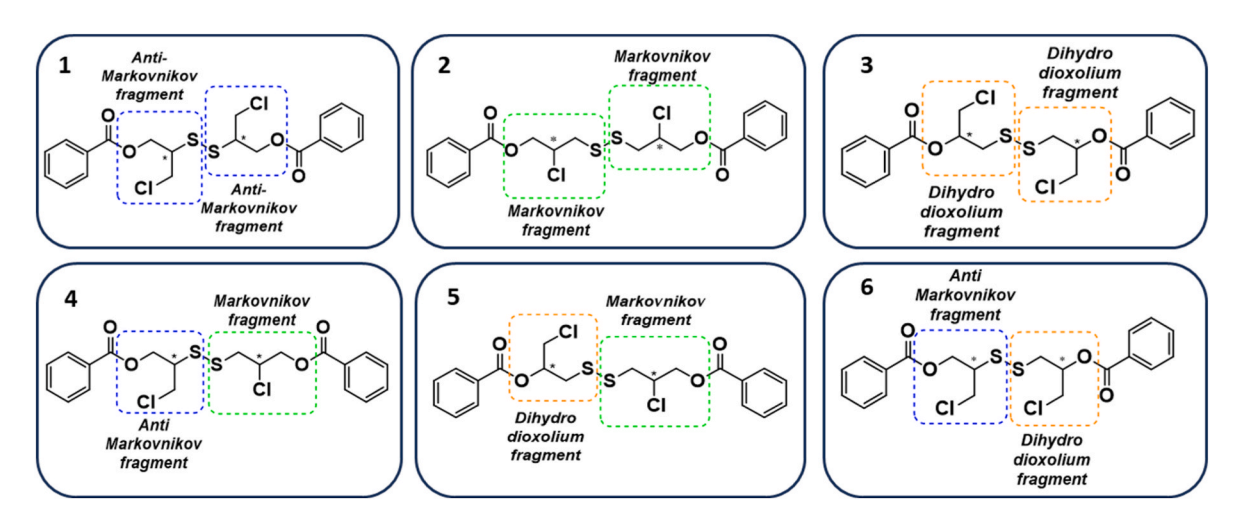
and grouping of different C–H nuclei into clusters in the HSQC cross peaks (Fig. 5) observed in further sections.

The stacked 1D ¹H NMR spectrum of the products for the reaction between allyl benzoate and Ph-S-Cl (Fig. 3a) was compared to the ¹H NMR spectra of both S₂Cl₂/allyl benzoate addition product mixtures (Fig. 3b) and poly(S₂-DAI-Cl₂) (Fig. 3c). The ¹H NMR spectrum of the product mixture of allyl benzoate and Ph-S-Cl was reasonably resolved and assignment of protons in the anti-Markovnikov -CH₂-Cl/-CH-S- and Markovnikov -CH-Cl/-CH₂-S- fragments/isomeric products were conducted by recognizing the chemical shift differences from H_x -C-S ($\delta \sim$ 3.3–3.7) vs H_x -C-Cl ($\delta \sim 3.8$ –4.2) moieties (Fig. 3a), and ¹³C DEPT NMR spectroscopy to resolve carbon atoms with methylene vs methine protons. The molar ratios of anti-Markovnikov (65%) vs Markovnikov (35%) isomeric products were discernible by the integration of -CH-Cl methine protons (H_d, $\delta = 4.24$; Fig. 3a) and -CH₂S- methylene protons $(H_a, \delta = 3.37; Fig. 3a)$ arising from the Markovnikov product (Scheme 2a) vs the –CH–S- methine proton (H_b, δ = 3.6; Fig. 3a) and the –CH₂-Cl methylene protons (H_c , $\delta = 3.79$ Fig. 3a) of the anti-Markovnikov

product (1:1.9). The methylene protons from the $-\text{OCH}_2$ - fragment (H_e , $\delta=4.62$; Fig. 3a) from both the Markovnikov and the anti-Markovnikov products from the monofunctional model reaction were overlapped and non-resolvable however, other peaks from both the Markovnikov product (H_a , $\delta=3.4$ and H_d $\delta=3.4$ 4.2, Fig. 3a) and the anti-Markovnikov product (H_b , $\delta=3.6$ and H_c , $\delta=3.8$; Fig. 3a) were sufficiently resolved to allow integration of proton peaks for quantitation of molar ratios. The Markovnikov (35-mol%) and anti-Markovnikov (65-mol%) products as shown in Scheme 2a provided insights into the complex proton resonances observed in the 1H NMR spectra of the poly (S_2 -DAI-Cl₂) made from SC-IV. However, proton peaks and fragments from the dihydrodioxolium pathway was not observed in the reaction of Ph-S-Cl and allyl benzoate as noted by the absence of downfield methine protons (H_f , $\delta=5.38$ –5.59; Fig. 3c) observed in the poly(S_2 -DAI-Cl₂) presumably due to steric effects from the phenyl group on Ph-S-Cl.

Analysis of the 1 H NMR spectrum of the allyl benzoate/ S_2 Cl₂ product mixture exhibited nearly exact proton resonance profiles of chemical shifts and peak clusters as for the poly(S_2 -DAI-Cl₂) for $H_{a'}$, $H_{c'}$, $H_{d'}$, and

Fig. 1. Proposed mechanistic pathways for the formation of products resulting from sulfur monochloride addition to allyl benzoate model compound.



 $\textbf{Fig. 2.} \ \, \textbf{Structures of all six regioisomers from allyl benzoate-} S_2 \textbf{Cl}_2 \, \textbf{model compound showing the component microstructure fragments for each regioisomeric dimer.} \\$

 $H_{e^{\cdot}}$ resonances (Fig. 3b, c). Notably, a distinct cluster of downfield proton resonances ($H_{f^{\cdot}}, \delta = 5.38-5.59$; Fig. 3b) were now observed in the allyl benzoate/ S_2Cl_2 product mixture, which tracked with dihydrodioxolium regioisomeric products as seen for the poly(S_2 -DAI-Cl₂) (Fig. 3c) and confirmed that S_2Cl_2 and allyl benzoate was the more useful model reaction for NMR structural analysis vs the allyl benzoate/Ph-S-Cl reaction pair. A key distinction in the 1H NMR spectrum of the S_2Cl_2 -allyl benzoate dimeric mixture is the introduction of another set of $-CH_2$ -Cl and $-CH_2$ -S protons from dihydrodioxolium regioisomers, which overlapped with these analogous set of protons from the Markovnikov and anti-Markovnikov products further complicating quantitative interpretation of these NMR spectra. Diastereotopism in the methylene protons ($H_{a^{\cdot}}$, $H_{c^{\cdot}}$, and $H_{e^{\cdot}}$; Fig. 3b) resulted in overlapping unresolved peaks between the methine proton -CH-S- ($H_{b^{\cdot}}$, $\delta = 3.40$ –3.65, Fig. 3b) of the anti-Markovnikov product and the methylene

protons –CH₂-S- (H_{a'}, $\delta=3.05$ –3.40, Fig. 3b) of the Markovnikov and dihydrodioxolium product. Poor resolution of overlapped resonances was also problematic for methine –CH–Cl protons (H_{d'}, $\delta=4.36$ –4.55, Fig. 3b) of the Markovnikov product and the methylene –CH₂-O- protons (H_{e'}, $\delta=4.53$ –4.70 ppm) of the Markovnikov and anti-Markovnikov products (Fig. 3b).

These poor resolution of key proton resonances in the ¹H NMR spectrum of the allyl benzoate-S₂Cl₂ model reaction impeded unambiguous proton assignments and quantification of the regioisomeric products from the electrophilic addition reaction. Hence, alternative NMR spectroscopic methods were required to complete the analysis of the allyl benzoate-S₂Cl₂ product mixture and poly(S₂-DAI-Cl₂), namely 2D NMR spectroscopic experiments such as Heteronuclear Single Quantum Coherence (HSQC), homonuclear Coherence Spectroscopy (COSY), and Heteronuclear Multiple Bond Correlation Spectroscopy

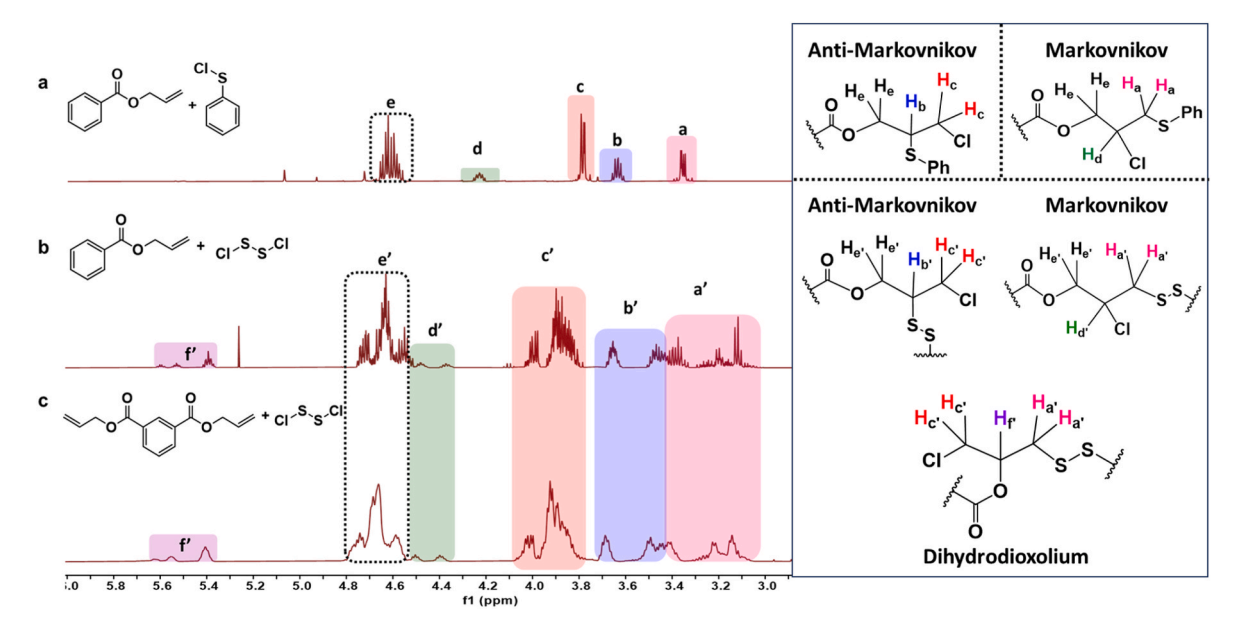


Fig. 3. 1 H NMR spectrum of model compound made from (a) allyl benzoate and phenyl sulfenyl chloride, (b) allyl benzoate and $S_{2}Cl_{2}$, (c) compared to the polymer from diallyl isophthalate and $S_{2}Cl_{2}$.

(HMBC) were carried out to further elucidate the microstructure of the allyl benzoate- S_2Cl_2 model compound, as discussed below.

Enhanced spectral resolution was obtained following the superimposition of the $^1\mathrm{H}$ spectrum (Fig. 3b) with the $^{13}\mathrm{C}$ spectrum (SeeSI Figure S6) as achieved by contour plots of 2D HSQC NMR spectroscopy of the allyl benzoate-S₂Cl₂ product mixture, facilitating the unequivocal assignment of overlapped $^1\mathrm{H}$ peaks (Fig. 4a). Initial observations of the 2D HSQC NMR spectroscopy oblique plots (Fig. 5) unveiled the presence

of cross peaks in clusters where the methine –CHS–, -CHCl, and –CHO–cross peaks were resolved as positive phased peaks (in yellow, Fig. 5a) and methylene –CH $_2$ S-, –CH $_2$ Cl and –CH $_2$ O- cross peaks as negative phased peaks (in blue, Fig. 5a) as commonly observed in 1D 13 C-DEPT NMR spectroscopy. The 2D HSQC NMR oblique plots delineate the full (Fig. 5a) and split (Fig. 5b and c) representation of cross peak clusters depending on their phase, followed by grouping of these cross peaks into fragments based on chemical shift contingent on the electronegativity of

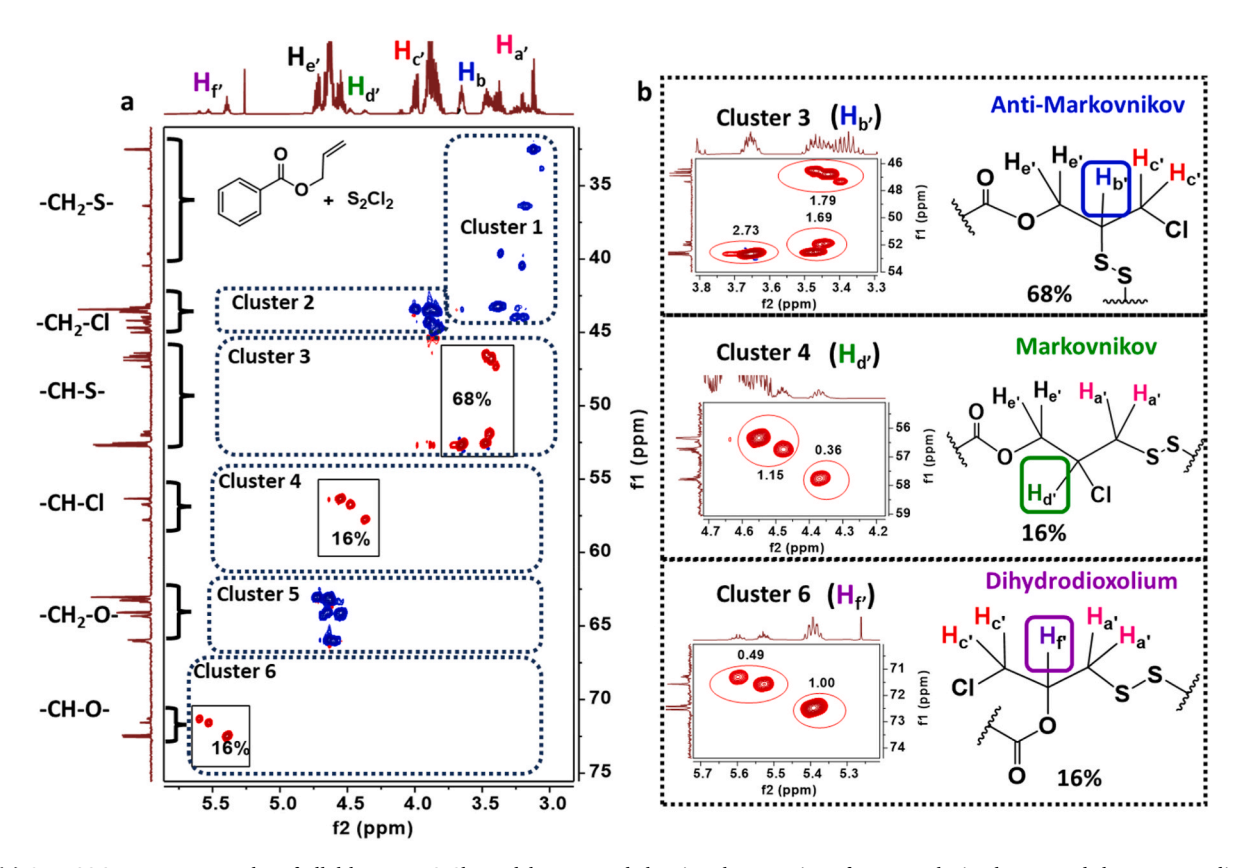


Fig. 4. (a) 2D HSQC NMR contour plot of allyl benzoate-S₂Cl₂ model compound showing the grouping of cross peaks in clusters and the corresponding carbon fragments and proton assignments, (b) methine clusters in order of increasing chemical shift and corresponding microstructure with proton highlighted.

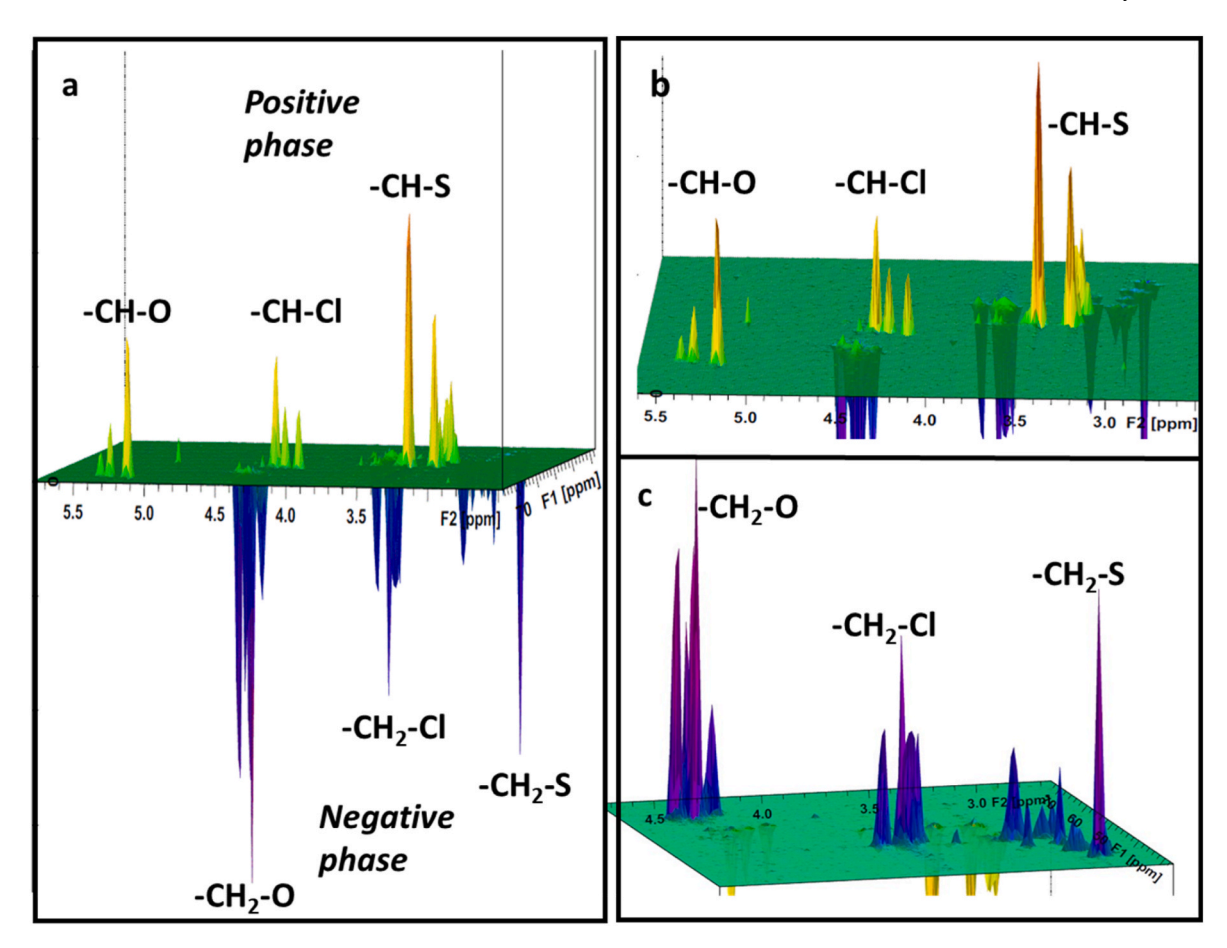


Fig. 5. (a) Oblique representation of the 2D HSQC NMR of the product mixture composition resulting from allyl benzoate and S_2Cl_2 showing the cross peaks in phases and clusters with fragment assignation for each cluster, **(b)** Positive phase of the 2D oblique HSQC for allyl benzoate- S_2Cl_2 product mixture showing the methine clusters and their molecular fragment, **(c)** and negative phase of the 2D oblique HSQC for allyl benzoate- S_2Cl_2 product mixture composition showing the methylene clusters and their molecular fragments.

the heteroatom attached to either the methylene or methine carbons. Grouping of cross peaks within a chemical shift range of 0.4 ppm along the $^{1}\mathrm{H}$ dimensions and 10 ppm range along the $^{13}\mathrm{C}$ dimension into clusters was done to enable assignment of C–H nuclei from the various Markovnikov, anti-Markovnikov and dihydrodioxolium regioisomeric fragments with equal consideration given to both the $^{1}\mathrm{H}$ and the $^{13}\mathrm{C}$ chemical shifts. Detailed carbon peak assignment following $^{13}\mathrm{C}\text{-DEPT}$ NMR experiments are listed in the supplementary information (See SI Table 1 and Fig. S6). This collective assessment of chemical shift and phase from both contour and oblique plots of the 2D HSQC NMR spectroscopy of the allyl benzoate/S2Cl2 product mixture was the first step in assigning cross peaks into clusters for subsequent analysis of regioisomeric product ratios as discussed below.

The contour representation of the 2D HSQC for the allyl benzoate-S₂Cl₂ model reaction product mixture (Fig. 4) was analyzed for chemical shifts (in conjunction with phase assignment of –CH₂- vs –CH– carbons from Fig. 5) and regioisomer microstructure quantification by integration of unique methine cross-peaks as will be discussed below. To enable more convenient assignment and discussion of C–H nuclei assignment to different regioisomeric products, grouping of cross peaks into six discrete clusters was conducted for the contour plots of the 2-D HSQC NMR spectrum of the allyl benzoate-S₂Cl₂ product mixture. Cluster 1 (1 H δ = 3.05–3.4; 13 C δ = 32.51–40.38; Fig. 4a) contains cross peaks for the methylene protons (H_a·; Fig. 5a) and carbons attached to the sulfur atom (-CH₂-S-) of the Markovnikov and dihydrodioxolium isomeric fragments. Cluster 2 (1 H δ = 3.80–4.00; 13 C δ = 42.97–44.98; Fig. 5a) contains the cross peaks of the methylene protons (H_c·; Fig. 5a) and carbons attached to the chlorine atom (-CH₂-Cl) of the anti-

Markovnikov and dihydrodioxolium isomeric fragments. The anti-Markovnikov isomeric fragment containing the methine protons (H_b Fig. 4a) and carbons attached to the sulfur atom (-CH-S-) was assigned to Cluster 3 (¹H $\delta = 3.4-3.65$; ¹³C δ (ppm) 46.37–52.75; Fig. 4a) while the Markovnikov isomeric fragment containing the methine protons (H_d; Fig. 4a) and carbons attached to the chlorine atom (-CH-Cl) was assigned to Cluster 4 (${}^{1}\text{H}\ \delta = 4.36\text{--}4.55$; ${}^{13}\text{C}\ \delta = 56.27\text{--}57.75$; Fig. 4a). Cluster 5 (${}^{1}H \delta = 4.53 - 4.70$; ${}^{13}C \delta = 63.03 - 66.04$; Fig. 4a) contains the cross peaks for the methylene protons (He; Fig. 4a) and carbons attached to the oxygen atom (-CH2-O-) of the anti-Markovnikov and Markovnikov isomeric fragments, while the most downfield cluster, Cluster 6 (¹H $\delta = 5.38-5.59$; ¹³C $\delta = 71.29-72.54$; Fig. 4a) contains the cross peaks for the methine protons (H_f; Fig. 4a) and carbons attached to the oxygen atom (-CH-O-) representing the dihydrodioxolium isomeric fragment. A ¹H⁻¹H 2D COSY experiment was also conducted on the allyl benzoate/ S₂Cl₂ product mixture to confirm proton correlations and interaction of fragments assigned to each Markovnikov, anti-Markovnikov and dihydrodioxolium regioisomer proposed in Fig. 2 (See SI Figure S7). In the COSY NMR experiment of the allyl benzoate/S2Cl2 product mixtures, the methine protons of the -CHS-, -CHCl and -CHO- from each regioisomer were particularly useful to map ¹H–¹H correlations with the two methylene protons from each regioisomeric moiety. Using these COSY NMR spectroscopic correlations, Cluster 3 methine protons/cross peaks $(H_b, ^1H \delta = 3.4-3.65; Fig. 4b)$ were assigned to the anti-Markovnikov isomeric fragment (-CH_b,-S-) due to the ¹H-¹H correlation with methylene protons ($H_{c'}$ $\delta = 3.80-4.00$; Fig. 4a) and ($H_{c'}$, ¹H $\delta = 4.53-4.70$; Fig. 4a) from Clusters 2 and 5 respectively (see SI Figure S7). Similarly, $^{1}\text{H}_{-}^{1}\text{H}$ COSY NMR correlation analysis for Cluster 4 protons (H_{d'}, $\delta =$

4.36–4.55; Fig. 4b) revealed interactions with <u>Cluster 1</u> methylene protons ($H_{a'}$, $\delta=3.05–3.4$; Fig. 4a) and <u>Cluster 5</u> methylene protons ($H_{e'}$, $\delta=4.53–4.70$; Fig. 4a) which collectively constituted the fragments for the Markovnikov regioisomer, while ${}^1H^{-1}H$ correlation with <u>Cluster 1</u> methylene protons ($H_{a'}$ ($\delta=3.05–3.4$; Fig. 4a), and <u>Cluster 2</u> methylene protons ($H_{c'}$, $\delta=3.80–4.00$; Fig. 4a) was correlated for <u>Cluster 6</u> methine protons (H_f , $\delta=5.38–5.59$; Fig. 4b) constituting the dihydrodioxolium regioisomer (SI Figure S7).

Using the same analytical methodology with 2D HSQC and COSY NMR spectroscopy, solution NMR spectroscopy of the poly(S_2 -DAI-Cl $_2$) can be conducted to both assign all cross peaks and integrate the 2D HSQC cross peaks from critical well-resolved methine fragments from Markovnikov, anti-Markovnikov and dihydrodioxolium regioisomeric moieties to quantify the molar ratios of units in the final polyhalodisulfide.

With full cross peak assignment from 2D HSQC and COSY NMR spectroscopy of the allyl benzoate/S₂Cl₂ product mixture, integration of discrete methine cross peaks from <u>Clusters 3,4 & 6</u> in Fig. 4b yielded the molar ratio of each of the Markovnikov, anti-Markovnikov and dihydrodioxolium regioisomeric units in the dimeric product mixture. For this analysis, the integration of <u>Cluster 3</u> methine cross peaks (C-H_b', ¹H δ (ppm) 3.4–3.65; ¹³C δ (ppm) 46.37–52.75; Fig. 4b) which represents the cross peaks of anti-Markovnikov microstructure fragment (CH_b·S-) contributed to 68% of the total regioisomer composition while the Markovnikov microstructure fragment (CH_d·Cl) represented by <u>Cluster 4</u> cross peaks (C-H_d', ¹H δ = 4.36–4.55; ¹³C δ = 56.27–57.75; Fig. 4b) and dihydrodioxolium microstructure fragment (CH_f-O-) depicted by <u>Cluster 6</u> cross peaks (C-H_f', ¹H δ = 5.38–5.59; ¹³C δ = 71.29–72.54; Fig. 4b) contributed 16% each to the total regioisomer composition.

Full cross peak assignment from 2D C–H HSQC and ¹H–¹H COSY NMR spectroscopy was conducted exactly as described in Figs. 1–5 on the poly(S₂-DAI-Cl₂) to quantify the molar ratios of Markovnikov, anti-

Markovnikov and dihydrodioxolium microstructures in the poly(S2-DAI- Cl_2) (M_n = 15,960 g/mol; M_w/M_n = 1.42) prepared by SC-IV in solution at T = 50 $^{\circ}$ C, which was isothermal to the conditions for the model reaction. 2D HSQC NMR contour plots of the poly(S2-DAI-Cl2) (Fig. 6a) exhibited very similar spectral features as with the allyl benzoate/S2Cl2 model reaction product mixture, with six major clusters of cross peaks as shown in Fig. 4. With all of the cross peak assignments for each regioisomeric fragment now able to be determined by comparison with the 2D NMR spectroscopic analysis for the small molecule model reactions, quantification of the Markovnikov, anti-Markovnikov and dihydrodioxolium microstructure units in the polymer was conducted by resolved methine cross peaks from each of these episulfonium ringopening pathways. The ratio of regioisomeric fragments obtained for the model compound closely agrees with that obtained for the polymer poly(S2-DAI-Cl2) synthesized at the same temperature (50 °C) where Cluster 3 methine protons ($H_{b'}$, ¹H $\delta = 3.46-3.75$; ¹³C $\delta = 46.46-52.75$; Fig. 6b) which constituted the anti-Markovnikov fragment (-CH_b,-S-) was the major regioisomeric microstructure (70-mol%) observed from this polymerization. Cluster 4 methine protons ($H_{d'}$, ¹H $\delta = 4.40-4.58$; 13 C $\delta = 56.27-57.75$; Fig. 6b) was assigned to the Markovnikov fragment (-CH_d-Cl) which when integrated constituted a minor regioisomeric microstructure (15-mol%), while Cluster 6 methine protons (H_f , $^1H \delta =$ 5.42–5.63; 13 C $\delta = 71.29–72.92$; Fig. 6b) constituted the dihydrodioxolium fragment (-CHf-O-) was also found to form a minor regioisomeric microstructure (15-mol%). The proposed poly(S2-DAI-Cl₂) microstructure of the polymer prepared by SC-IV at 50 °C is presented in Fig. 7, along with the 2D HSQC NMR oblique plots showing as positively phased peaks the key -CH_b'-S-, -CH_d'-Cl, -CH_f-O- methine cross peaks that were essential to the structural quantification of the different microstructures. We also note the small temperature dependence of SC-IV on the microstructure composition of poly(S2-DAI-Cl2) as polymer prepared at slightly higher temperature (T = 70 °C) affords

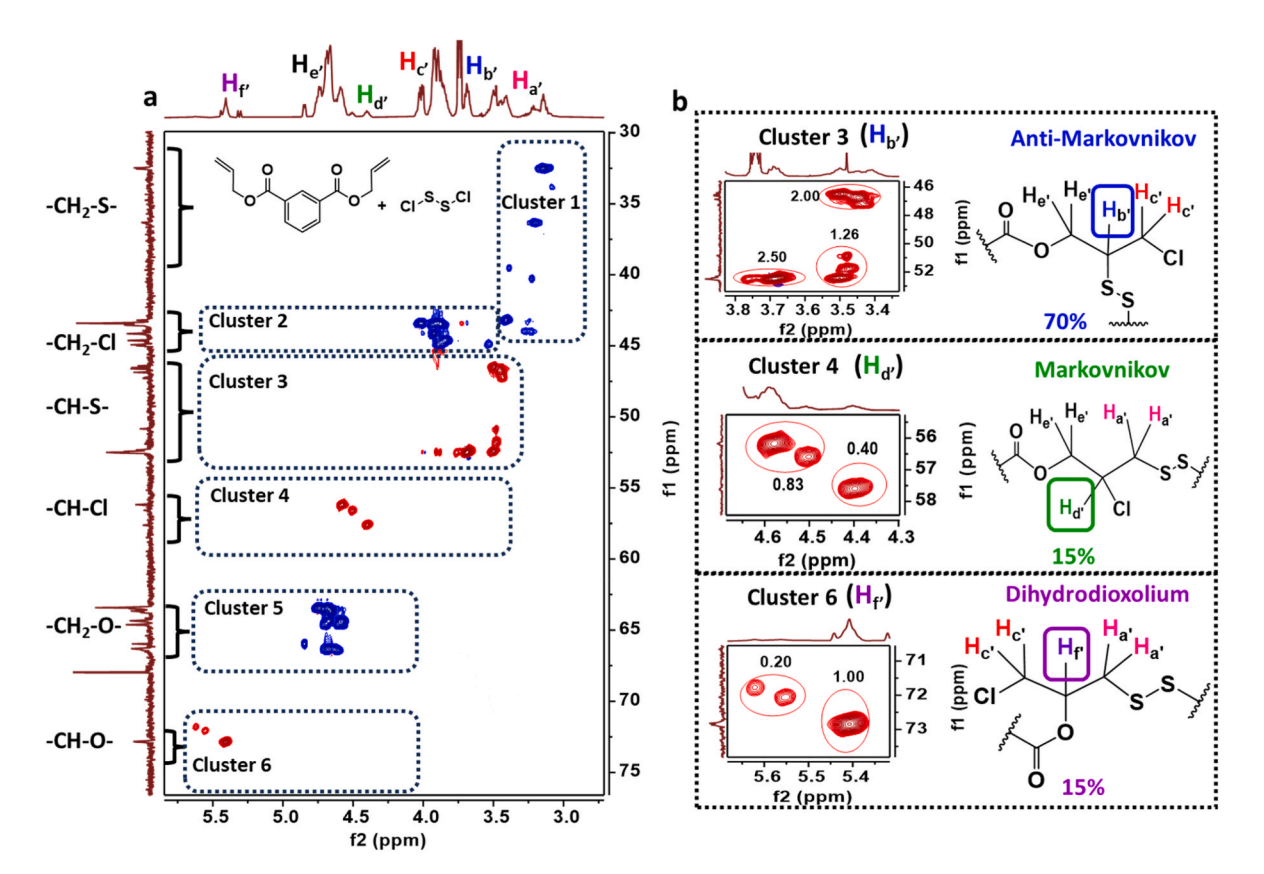


Fig. 6. (a) 2D HSQC of poly(S₂-DAI-Cl₂) showing the grouping of cross peak in clusters and the corresponding carbon fragments and proton assignments, (b) methine clusters in order of increasing chemical shift and corresponding microstructure with proton highlighted.

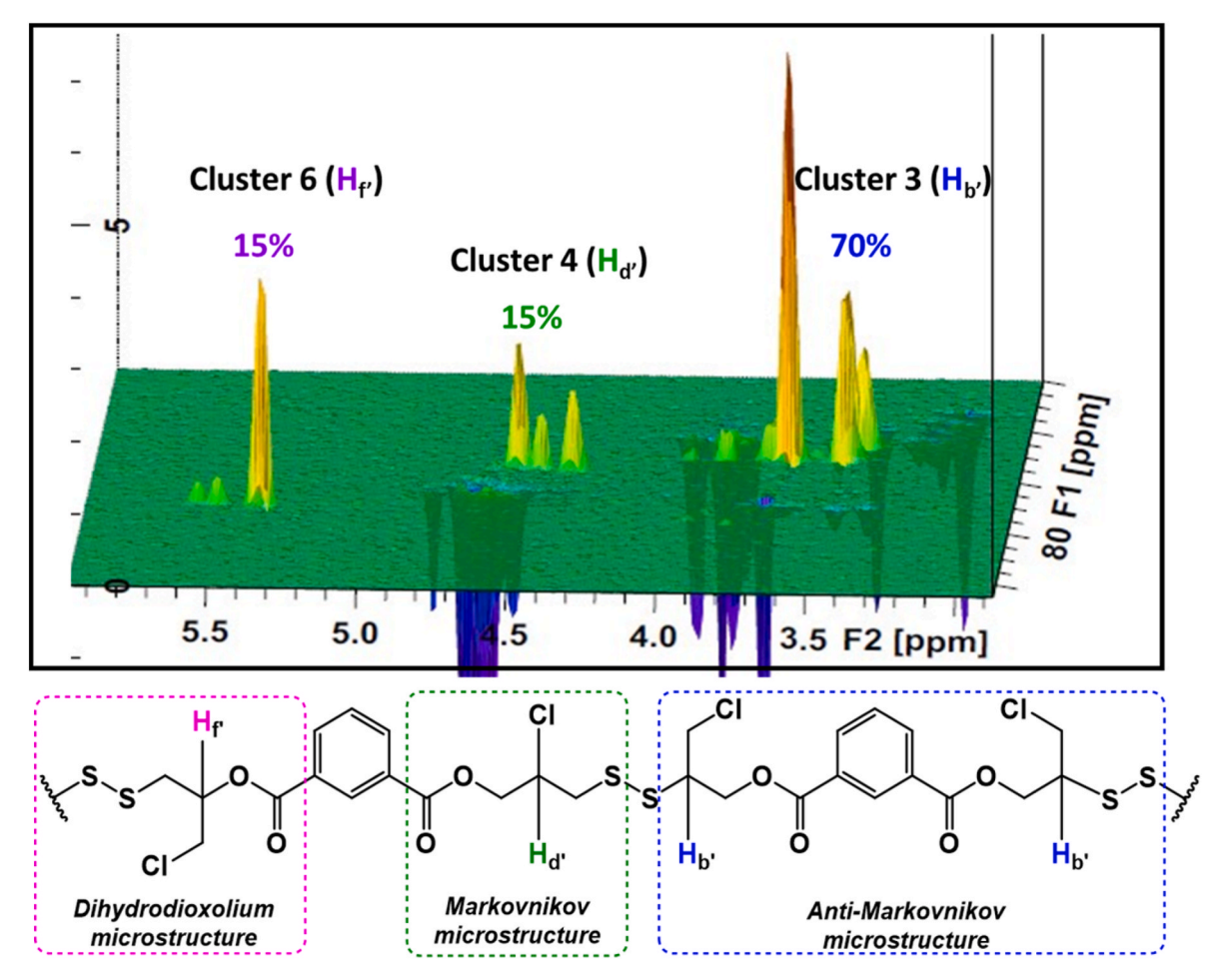


Fig. 7. (a) 2D HSQC NMR oblique plot of positively phased of well resolved -CH_b·-S-, -CH_d·-Cl, (-CH_f-O- methine cross peaks used to quantify the microstructure composition and regioisomer quantification of poly(S_2 -DAI-Cl₂) prepared by SC-IV in solution at T = 50 °C (b) poly(S_2 -DAI-Cl₂) microstructures and molar ratios of each regioisomeric unit.

slight enrichment of the Markovnikov (17%) and the dihydrodioxolium (23%) microstructure units and a lower composition for the anti-Markovnikov microstructure (60%). These NMR spectroscopic methodology allowed for facile comparison of changes to poly(S₂-DAI-Cl₂) regioisomeric unit molar ratios as a function of SC-IV temperature, where significant reduction of anti-Markovnikov microstructure units was observed at higher reactions temperatures ($T \ge 90$ °C, Table 1; and Supporting Information Figs. S12–17).

3. Conclusion

Comprehensive structural characterization of polyhalodisulfides prepared via sulfenyl chloride inverse vulcanization, specifically focusing on regiosiomeric units from the polymerization of 1,3-diallyl isophthalate and S_2Cl_2 , is reported for the first time using 1-D and 2D NMR spectroscopy. ¹H NMR, ¹³C NMR, 2D HSQC, and 2D COSY spectroscopic analysis were carried out on the products of model compounds

Table 1
The effect of temperature on the distribution of the microstructures.

Polymerization temperature	Methine proton distribution (%)		
	-CH-O-	-CH-Cl	-CH-S-
50 °C	14.7	14.8	69.5
60 °C	21.4	17.3	61.3
90 °C	24.5	21.2	54.3
120 °C	24.8	30.5	44.7

for these SC-IV polymerizations. We report on an analytical method to quantify the regioisomeric product ratios formed by different episulfonium intermediate ring-opening pathways and demonstrate how 2D NMR spectroscopic technique can be used to integrate key cross peaks for this analysis for the first time. Furthermore, we discuss how poly(S2-DAI-Cl2) regioisomeric microstructures can be quantified using this NMR spectroscopic method. This report presents significant advance to accelerate structural characterization of polyhalodisulfides made by sulfenyl chloride inverse vulcanization of allylic esters, which will be a central tool in mapping structure-property effect of polyhalodisulfide regiochemistry on bulk thermomechanical polymer properties.

CRediT authorship contribution statement

Chisom Olikagu: Conceptualization, Data curation, Formal analysis, Investigation, Methodology, Validation, Visualization, Writing – original draft, Writing – review & editing. Vlad K. Kumirov: Data curation, Formal analysis. Jon T. Njardarson: Data curation, Formal analysis. Megan J. Hahn: Investigation. Jeffrey Pyun: Conceptualization, Funding acquisition, Supervision, Writing – original draft, Writing – review & editing.

Declaration of competing interest

The authors declare the following financial interests/personal relationships which may be considered as potential competing interests: Jeffrey Pyun reports financial support was provided by National Science Foundation. If there are other authors, they declare that they have no known competing financial interests or personal relationships that could have appeared to influence the work reported in this paper.

Data availability

Data will be made available on request.

Acknowledgements

We gratefully acknowledge the National Science Foundation (CHE-2201155) for support of this work.

Appendix A. Supplementary data

Supplementary data to this article can be found online at https://doi.org/10.1016/j.polymer.2023.126539.

References

- [1] K.-S. Kang, C. Olikagu, T. Lee, J. Bao, J. Molineux, L.N. Holmen, K.P. Martin, K.-J. Kim, K.H. Kim, J. Bang, V.K. Kumirov, R.S. Glass, R.A. Norwood, J.T. Njardarson, J. Pyun, Sulfenyl chlorides: an alternative monomer feedstock from elemental sulfur for polymer synthesis, J. Am. Chem. Soc. 144 (50) (2022) 23044–23052, https://doi.org/10.1021/jacs.2c10317.
- [2] J.J. Griebel, R.S. Glass, K. Char, J. Pyun, Polymerizations with elemental sulfur: a novel route to high sulfur content polymers for sustainability, energy and defense, Prog. Polym. Sci. 58 (2016) 90–125, https://doi.org/10.1016/j. prographymsci.2016.04.003
- [3] M.J.H. Worthington, R.L. Kucera, J.M. Chalker, Green chemistry and polymers made from sulfur, Green Chem. 19 (12) (2017) 2748–2761, https://doi.org/ 10.1039/C7GC00014F
- [4] J.M. Chalker, M.J.H. Worthington, N.A. Lundquist, L.J. Esdaile, Synthesis and applications of polymers made by inverse vulcanization, Top. Curr. Chem. 377 (16) (2019) 1–27, https://doi.org/10.1007/s41061-019-0242-7.
- [5] Y. Zhang, R.S. Glass, K. Char, J. Pyun, Recent advances in the polymerization of elemental sulfur, inverse vulcanization and methods to obtain functional chalcogenide hybrid inorganic/organic polymers (CHIPS), Polym. Chem. 10 (30) (2019) 4078–4105, https://doi.org/10.1039/C9PY00636B.
- [6] T. Lee, P.T. Dirlam, J.T. Njardarson, R.S. Glass, J. Pyun, Polymerizations with elemental sulfur: from petroleum refining to polymeric materials, J. Am. Chem. Soc. 144 (1) (2022) 5–22, https://doi.org/10.1021/jacs.1c09329.
- [7] W.J. Chung, J.J. Griebel, E.T. Kim, H. Yoon, A.G. Simmonds, H.J. Ji, P.T. Dirlam, R. S. Glass, J.J. Wie, N.A. Nguyen, B.W. Guralnick, J. Park, Á. Somogyi, P. Theato, M. E. Mackay, Y.-E. Sung, K. Char, J. Pyun, The use of elemental sulfur as an alternative feedstock for polymeric materials, Nat. Chem. 5 (2013) 518–524, https://doi.org/10.1038/nchem.1624.
- [8] Y. Zhang, K.M. Konopka, R.S. Glass, K. Char, J. Pyun, Chalcogenide hybrid inorganic/organic polymers (CHIPs) via inverse vulcanization and dynamic

- covalent polymerizations, Polym. Chem. 8 (34) (2017) 5167–5173, https://doi.org/10.1039/C7PY00587C.
- [9] Y. Zhang, T.S. Kleine, K.J. Carothers, D.D. Phan, R.S. Glass, M.E. Mackay, K. Char, J. Pyun, Functionalized chalcogenide hybrid inorganic/organic polymers (CHIPs) via inverse vulcanization of elemental sulfur and vinylanilines, Polym. Chem. 9 (17) (2018) 2290–2294, https://doi.org/10.1039/C8PY00270C.
- [10] Y. Zhang, N.G. Pavlopoulos, T.S. Kleine, M. Karayilan, R.S. Glass, K. Char, J. Pyun, Nucleophilic activation of elemental sulfur for inverse vulcanization and dynamic covalent polymerizations, J. Polym. Sci., Part A: Polym. Chem. 57 (1) (2019) 7–12, https://doi.org/10.1002/pola.29266.
- [11] X. Wu, J.A. Smith, S. Petcher, B. Zhang, D.J. Parker, J.M. Griffin, T. Hasell, Catalytic inverse vulcanization, Nat. Commun. 10 (2019) 647, https://doi.org/ 10.1038/s41467-019-08430-8.
- [12] L.J. Dodd, Ö. Omar, X. Wu, T. Hasell, Ivestigating the role and scope of catalysis in inverse vulcanization, ACS Catal. 11 (8) (2021) 4441–4455, https://doi.org/ 10.1021/acscatal.0c05010.
- [13] J.M.M. Pople, T.P. Nicholls, L.N. Pham, W.M. Bloch, L.S. Lisboa, M.V. Perkins, C. T. Gibson, M.L. Coote, Z. Jia, J.M. Chalker, J. Am. Chem. Soc. 145 (2023) 11798–11810, https://doi.org/10.1021/jacs.3c03239.
- [14] I.A. Abu-yousef, D.N. Harpp, New sulfenyl chloride chemistry: synthesis, reactions and mechanisms towards carbon-carbon double bonds, Sulfur Rep. 24 (3) (2003) 255–282, https://doi.org/10.1080/01961770308047977.
- [15] I.A. Abu-Yousef, The organic chemistry of diatomic sulfur, J. Sulfur Chem. 27 (1) (2006) 87–119, https://doi.org/10.1080/17415990600556349.
- [16] F. Rowlinson, Cold vulcanization of rubber, Sci. Am. 124 (1921) 369. http://www.jstor.org/stable/24979692.
- [17] J. Glazer, Dilatometric measurement of the rate of vulcanization of crêpe-rubber by sulfur monochloride, Nature 167 (1951) 404–405, https://doi.org/10.1038/ 167404b0.
- [18] F. Lautenschlaeger, Reation of sulfur dichloride with linear diolefins. Stereochemical aspects in the formation of cyclic sulfides, J. Org. Chem. 33 (7) (1968) 2620–2627, https://doi.org/10.1021/jo01271a003.
- [19] F. Lautenschlaeger, Reaction of sulfur dichloride with cyclic polyolefins, J. Org. Chem. 33 (7) (1968) 2627–2633, https://doi.org/10.1021/jo01271a004.
- [20] R.A. Meyers, E.R. Wilson, Copolymerization of sulfur monochloride with cyclopentadiene, Polym. Lett. 6 (1968) 587–591, https://doi.org/10.1002/ pol.1968.110060810.
- [21] R.A. Meyers, E.R. Wilson, A novel copolymerization reaction, Polym. Lett. 6 (1968) 531–534, https://doi.org/10.1002/pol.1968.110060714.
- [22] R.A. Meyers, J. Hom, Addition Copolymerization of sulfur dichloride and sulfur monochloride with 1,3-butadiene, J. Macromol. Sci., Chem. 3 (2) (1969) 169–176, https://doi.org/10.1080/10601326908053802.
- [23] J. Pielichowski, A new reaction of N-vinylcarbazole with disulfur dichloride, Angew. Chem., Int. Ed. 8 (11) (1969) 877–878, https://doi.org/10.1002/ anje.196908772.
- [24] J. Yoo, S.R. D'Mello, T. Graf, A.K. Salem, N.B. Bowden, Synthesis of the first poly (diaminosulfide)s and an investigation of their application as drug delivery vehicles, Macromolecules 45 (2) (2012) 688–697, https://doi.org/10.1021/ ma2023167.
- [25] S.M. Geary, Q. Hu, V.B. Joshi, N.B. Bowden, A.K. Salem, Diaminosulfide based polymer microparicles as cancer vaccine delivery systems, J. Contr. Release 220 (2015) 682–690, https://doi.org/10.1016/j.jconrel.2015.09.002.
- [26] K. Hu, W.M. Westler, J.L. Markley, Simultaneous qunatification and identification of individual chemicals in metabolite mixtures by two-dimensional extrapoltated time-zero ¹H-¹³C HSQC (HSQC₀), J. Am. Chem. Soc. 133 (6) (2011) 1662–1665, https://doi.org/10.1021/ja1095304.